Effect of shaft rotation of driven spiral piles on vertical bearing capacity

Takahiro Sato, Jun Otani, Bastien Chevalier, Tugba Eskisar

Effect of shaft rotation of driven spiral piles on vertical bearing capacity

Takahiro Sato [i], Jun Otani [ii], Bastien Chevalier [iii] and Tugba Eskisar [iv]

i) Technical Staff, X-Earth Center, Kumamoto University, 2-39-1 Kurokami, Kumamoto, 860-8555, Japan.
ii) Professor, X-Earth Center, Kumamoto University, 2-39-1 Kurokami, Kumamoto, 860-8555, Japan.
iii) Assistant Professor, Clermont Université, Université Blaise Pascal, Institut Pascal, Clermont-Ferrand, France.
iv) Researcher, Civil Engineering Department, Ege University, 35100 Bornova İzmir, Turkey.

ABSTRACT

This study explores the production of a new type of pile. This new spiral pile is made of a twisted steel plate, creating a continuous spiral shape. Before starting the large-scale production of these piles, it is necessary to experimentally determine their bearing qualities, which are related to installation method. It is also necessary to develop an analytical model to determine their bearing capacity. The purpose of this study is to determine the bearing qualities of the spiral pile and the behavior of the surrounding ground. Considering this, the first objective is to examine the incidence of the shape of the pile. The installation method and penetration resistances are thoroughly discussed on the basis of the results of static loading tests using model piles. The static penetration tests were conducted under various shaft rotary conditions at the model pile head. It was confirmed that the shaft rotary condition has a significant impact on the penetration resistance and vertical bearing capacity of the spiral pile. The second objective is to show the behavior of the ground before and during penetration using X-ray computerized tomography (CT). An industrial X-ray CT scanner was used to observe changes in the density of the sand surrounding the spiral piles before and during penetration. The disturbance area of the ground surrounding the spiral pile was observed using CT images; the images revealed that the disturbance area surrounding the spiral pile was significantly affected by shaft rotary conditions.

Keywords: spiral pile, model tests, rotary installation, vertical bearing capacity, X-ray CT scanner

1 INTRODUCTION

The present general methods of casting foundation piles are classified on the basis of three sets of criteria: whether the piles are precast or cast-in-situ and whether they are driven or bored. Driven precast pile methods have the advantages of requiring little on-site construction, which shortens work periods and simplifies on-site construction control. Further, new pile foundations have been proposed, such as the rotary or jacking pile methods, which can reduce both the noise and vibration that occur during installation (Yamashita 2010, Isohata 2003).

In recent years, a new structural form has been developed for earth reinforcement. The new form is called a spiral bar and is produced by twisting a flat steel bar. The use of this structural material is expected to increase in the coming years. The researchers who proposed using spiral bars for earth reinforcement on embankments reported that the pullout resistance of the spiral bar is equivalent to or higher than that of a similarly inserted steel rod. Other spiral bar research consisted of basic material tests, laboratory tests, full-scale loading tests, and numerical analyses with a spiral pile as the ground reinforcement structure. The existing research primarily describes the characteristic pullout resistance, revealing the spiral bar's usefulness as a structural form and suggesting a formula to estimate its bearing capacity. However, the influence of the interaction between the spiral pile and the ground when driving the pile has not been well inspected because of difficulties in taking measurements. Although contributing factors such as the heterogeneity of the test ground and constructional failure are provided, researchers are yet to conclusively identify the causes (Hirata 2003, Hirata 2005). It is believed that the understanding of the detailed interactions between the pile and the ground would allow an advanced design method.

In this paper, penetration tests were conducted using model ground and varying a number of parameters, such as the shape of the pile, the density of the ground, and the method of installation. After confirming the basic bearing capacity with the penetration tests, the disturbed area of the model ground was observed using an industrial X-ray computerized tomography (CT) scanner. The effectiveness of the selected parameters

was thoroughly discussed on the basis of the results of the mechanical model test and the CT images.

2 STATIC INSTALLATION EXPERIMENT

Initially, a static vertical penetration test was conducted with model piles to gain a basic understanding of the vertical bearing capacity. Fig. 1 shows the model piles, and their dimensions are listed in Table 1. Three types of spiral piles, varying in the amount of torsion, were used to examine the relationship between pile shape and bearing capacity. To compare the bearing capacity of the spiral piles to the current commonly used forms, plate and tube piles were prepared. The spiral piles' variable of specific angle corresponded to the angle between a tangent lying along the edge of the pile and the horizontal plane. For the flat plate, the angle of the edge was 90° with respect to the horizontal plane, and the angle of the edge of the Spiral45 pile, which has the greatest torsion, was 45°. The name of each model spiral pile refers to its specific angle: Spiral76, Spiral64, and Spiral45. Fig. 2 shows each spiral pile's specific angle. The model piles are equal in length, width (width here describes both the width of the spiral plates before twisting and the diameter of the tube pile), and cross-sectional area. The pitch of the spiral pile is defined as the axial length required for one complete rotation.

Fig. 3 shows the soil box, model ground, and loading shaft. Dry Toyoura sand (D_{50} = 0.175 mm) was used for the model ground. The sand was packed in the soil box by using the raining method under the relative density condition of D_r = 44% to 82%. The loading shaft was designed to control the rotary condition of the model pile from the upper shaft. The aluminum cylinder in the upper shaft contained a ball bearing that linked the shaft to the loading machine so the shaft could turn smoothly. The spiral pile was fixed at the lower end of the shaft. Just under the aluminum cylinder, there was a clamping ring that could set the shaft rotary as locked or free.

Fig. 4 shows a summary of the test procedure. The static installation tests were compared for different ground conditions and shaft rotary conditions. The experiments were conducted with two phases of static penetration. The first phase, named the driving phase, simulated driving the pile foundation on-site. The second phase, named the loading phase, simulated the force exerted on the pile head by the loading weight of the construction. The load and the penetration depth were measured at the pile head. The velocity of penetration was 20 mm/min during the driving phase and 0.25 mm/min during the loading phase.

In this study, the static penetration tests were performed under different shaft rotary conditions at the pile head for the sake of comparison. The shaft rotary conditions were as follows: 1) Locked rotary condition: The pile was fixed to the loading shaft. 2) Free rotary condition: The model pile could rotate smoothly without loading shaft friction. 3) Forced rotary condition: The spiral pile was rotated by hand at a given rotation ratio. "Rotation ratio 100%" or "Rot 100%" means that during the installation, every section of the spiral pile would go through the ground in the exact same position. Thus, the pile would rotate once (360°) for each pitch length that it moved downward.

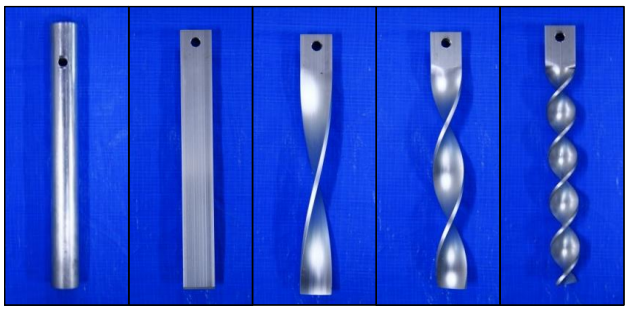

Fig. 1. Model piles.

Table 1. Dimensions of the model piles.

Pile shape	Tube	Plate	Spiral76	Spiral64	Spiral45
Length (mm)	145	145	145	145	145
Width (mm)	20	20	20	20	20
Thickness (mm)	1	3	3	3	3
Cross section (mm^2)	60	60	60	60	60
Pitch (mm)	-	-	260	130	62
Specific angle (°)	-	90	76	64	45

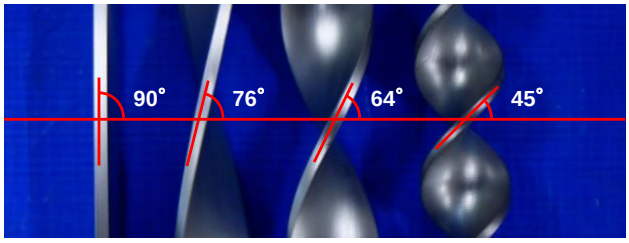

Fig. 2. Specific angles of the plate and spiral piles.

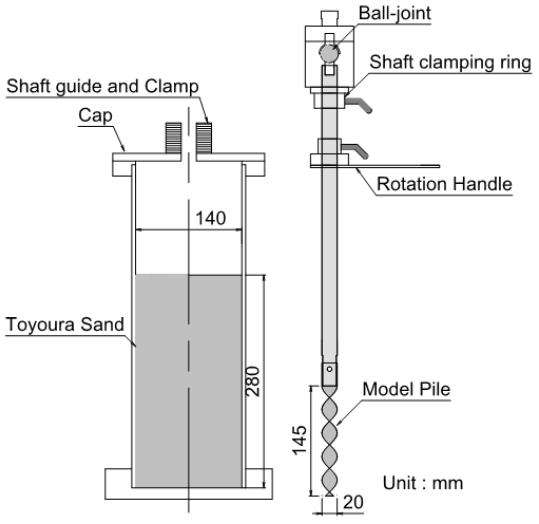

Fig. 3. Soil box, model ground, and loading shaft.

The test conditions for the driving and loading phases were abbreviated as well, e.g., "Free-Locked," which means a free rotary driving phase and a locked rotary loading phase. Table 2 shows the possible test conditions for each variable. The results of the forced rotary condition are presented in Section 4.

The relationship between the pile head load and the penetration depth is shown in Fig. 5 for the tube, plate, and Spiral45 piles. During the driving phase of the model piles, the plate pile generated the smallest penetration resistance. The tube pile and the Spiral45 pile in the locked rotary condition generated the largest resistance. The difference in the penetration resistance occurred due to the varied shapes of the piles. In the driving phase, the spiral pile in the free rotary condition generated a small resistance compared with the pile in the locked rotary condition. On the other hand, the amount of head load required to move the Spiral45 pile in the loading phase was much larger than in the driving phase in the Free-Locked condition. If the spiral pile had been driven with shaft rotation permitted, the penetration resistance would have reduced, but it worked best on service in the shaft locked condition. However, initial settlement would have occurred before a high bearing capacity was exhibited.

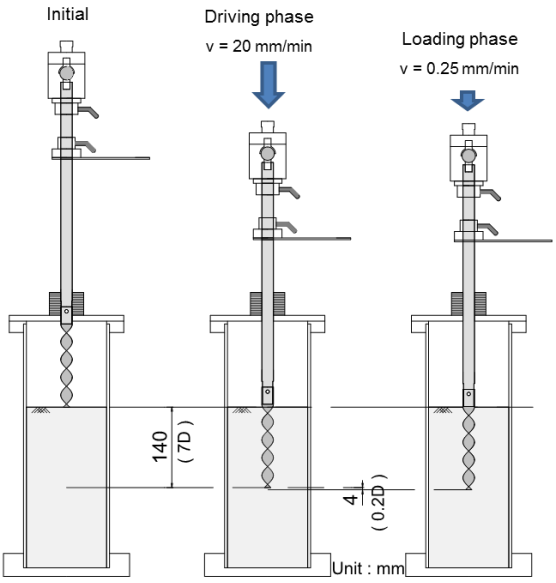

Fig. 4. Summary of the test procedure.

Table 2. Test conditions.

Rotary conditions (Driving phase)	Locked	Free	Rot.ratio 50%	Rot.ratio 100%	Rot.ratio 200%
Rotary conditions (Loading phase)	Locked		Free		
Model ground	44% ~ 82% (D_r : Relative density)				

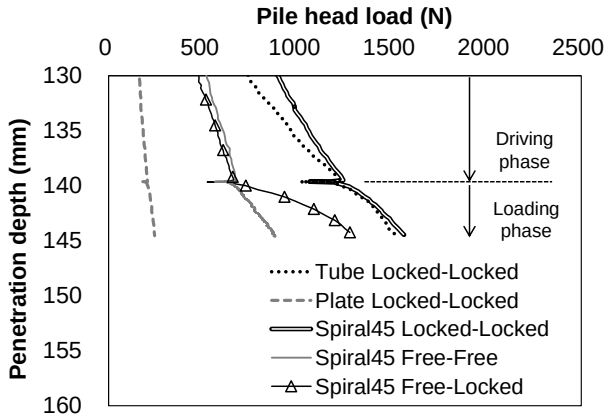

Fig. 5. Relationship between pile head load and penetration depth (Close-up of penetration depth after 130 mm).

3 FREE ROTARY INSTALLATION EXPERIMENT

In the static installation experiments of the model piles, it was confirmed that the penetration resistance was reduced by permitting the spiral pile to rotate. Thus, it can be inferred that there is a close relationship

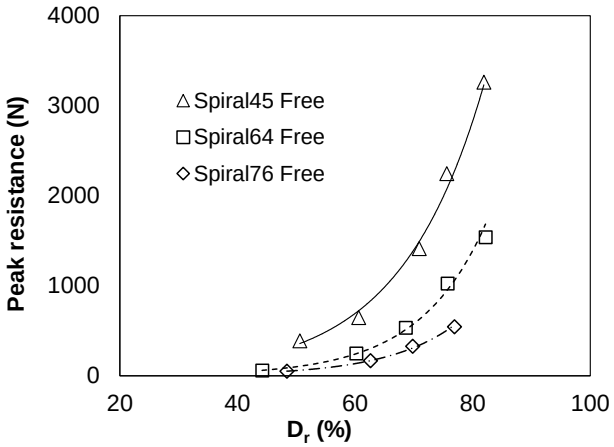

Fig. 6. Peak resistance of the driving phase (Free rotary condition).

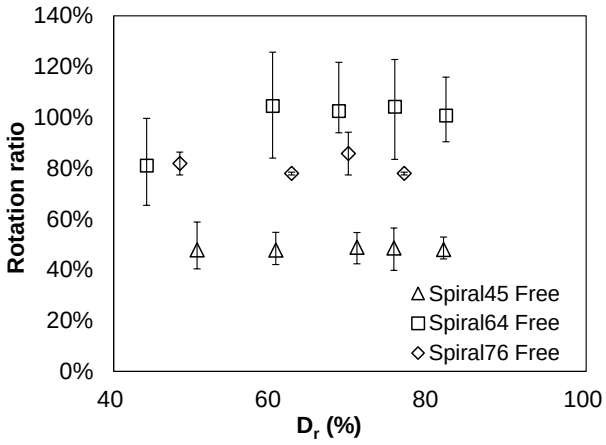

Fig. 7. Rotation ratio of model pile in the driving phase (Free rotary condition).

between the rotary condition and the penetration resistance of the spiral pile. Penetration tests were then conducted under the free rotary condition. These tests were conducted in the driving phase to compare the rotation ratios of different spiral piles. The rotation ratio is defined as the axial rotation over the interval where the length of one pitch of the model pile penetrates the ground divided by the specific angle of the pile. The tests were conducted with varying model ground densities and different spiral pile shapes. The dead load was applied across the whole ground surface to produce a high confining pressure simulating deep ground condition.

Fig. 6 shows the effect of ground density and spiral pile shape on the peak resistance during the driving phase, with all piles under the free rotary condition. For every model ground density, Spiral45 generated a high penetration resistance. These results indicate a correlation between the pile shapes and rotation ratios and their corresponding peak resistances. Fig. 7 shows the rotation ratio of each pile during the driving phase under the free rotary condition. For every model ground density, the rotation ratio of the Spiral45 pile was approximately 50%. In contrast, the rotation ratios of the Spiral64 and Spiral76 piles were approximately 100% and 80%, respectively. It can be inferred that the rotation ratio is very important in the generation of penetration resistance. As the pile is driven into the ground, the reactive force that the ground applies to the pile body during the driving phase produces a torque because of the shape of the pile. However, the pile simultaneously experiences resistance due to the friction of the ground–surface contact. The specific angle of the spiral pile essentially determines the rotation ratio in the free rotary condition. However, these are the results of a small, limited laboratory test, so additional experiments with more practical conditions are required to make definitive conclusions.

The penetration resistances of the Spiral64 and Spiral76 piles were not very high, and the rotation ratios of these two were nearly 100% in the free rotary condition. These spirals yielded results similar to those of the plate pile in the driving phase. On the other hand, the penetration resistance of the Spiral45 pile was several times higher than that of the other piles, and the rotation ratio was nearly 50%. From these results, it appears the penetration resistance of the spiral pile is strongly influenced by the rotation ratio. As the rotation ratio increases, the penetration resistance decreases. At the same time, it appears that the rotation ratio of the pile shape of Spiral45, which produces a great deal of torsion, cannot reach 100% during the spontaneous rotation of the free rotary condition. This would imply that bringing the pile rotation ratio close to 100% with the forced rotary condition would reduce the penetration resistance during the driving phase.

4 RELATIONSHIP BETWEEN ROTARY CONDITION AND RESISTANCE

Based on the results presented in Section 3, penetration tests were conducted while manually controlling the shaft rotary condition. The penetration resistance and the vertical bearing capacity were compared under different rotary conditions using the Spiral45 pile. Fig. 8 shows the influence of the rotation ratio on the peak resistance for a range of model ground densities, including both the spontaneous rotation ratio obtained under the free rotary condition and various rotation ratios under the forced rotary condition. The penetration resistance was inversely proportional to the rotation ratio, particularly with a high relative model ground density. The results of driving and loading phase tests under the forced rotary condition are shown in Fig. 9. In the driving phase, the penetration resistance when the rotation ratio was forced at 100% (Rot 100%) was reduced as compared to the free rotary condition. The Rot 100% condition generated a resistance lower than half of that of the locked rotary condition at an installation depth of 140 mm. The Rot

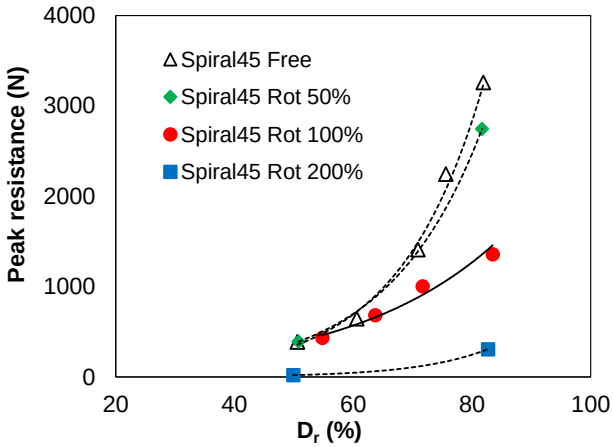

Fig. 8. Peak resistance during the driving phase as a function of rotation ratio.

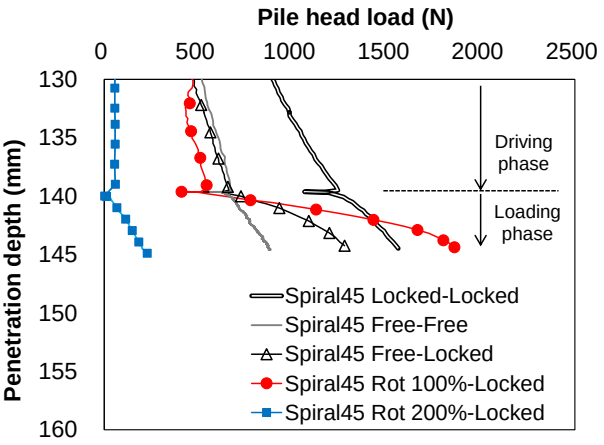

Fig. 9. Relationship between pile head load and penetration depth (Close-up of the penetration depth after 130 mm).

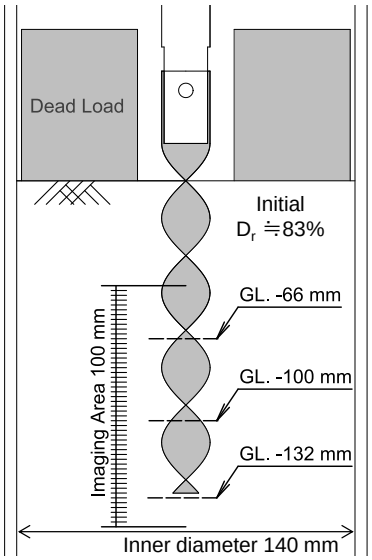

Fig. 10. Scanning area of X-ray CT.

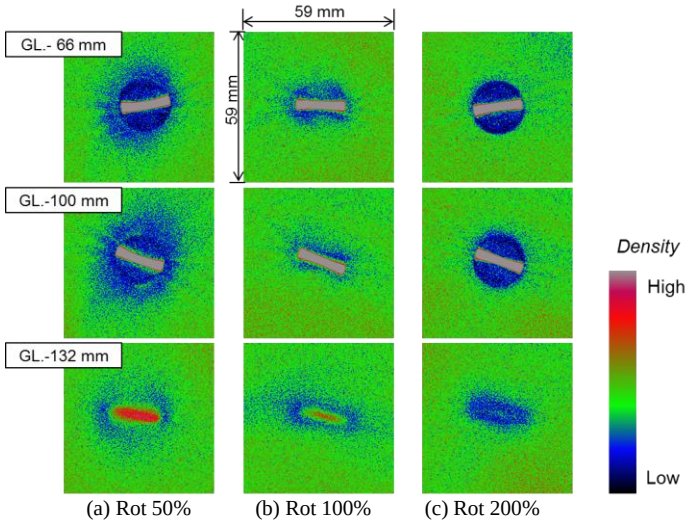

(a) Rot 50% (b) Rot 100% (c) Rot 200%

Fig. 11. Horizontal cross-sectional CT images.

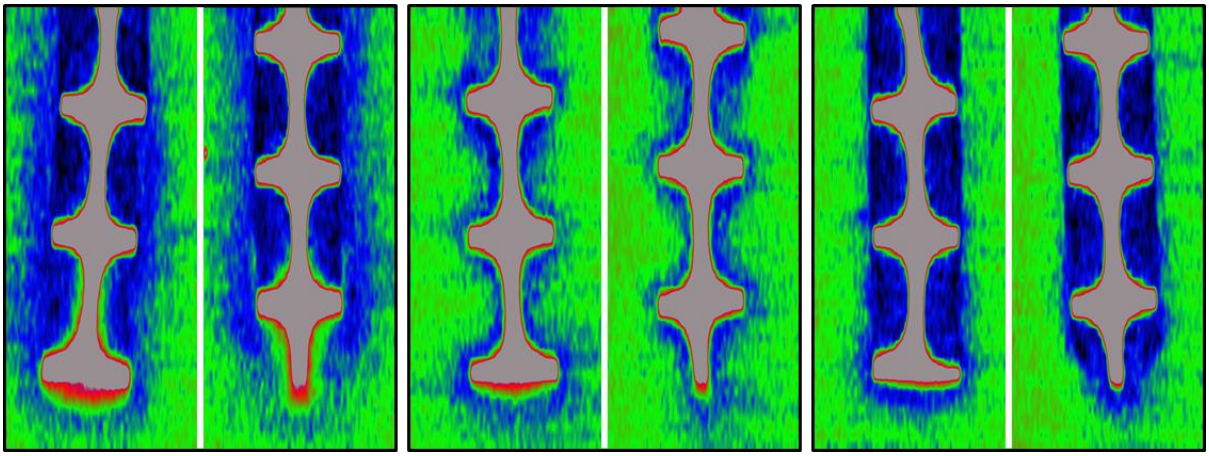

(a) Rot 50% (b) Rot 100% (c) Rot 200%

Fig. 12. Vertical cross-sectional CT images.

200% condition reduced the penetration resistance even further.

The penetration resistance was reduced by forcing shaft rotation, and it was confirmed that the amount of reduction was greatly influenced by the rotation ratio. Following the driving phase, the penetration resistance experienced a sharp increase under the locked rotary condition during the loading phase. This behavior was essentially similar to that in the Free-Locked installation experiment, but the increased rate of resistance was different for each rotation ratio. The case of Rot 100%-Locked yielded the greatest increase in the penetration resistance in the loading phase, surpassing the Locked-Locked condition when the amount that the pile settled reached 20% of the pile diameter (0.2D). It is important to maintain an optimum rotation ratio to reduce the penetration resistance and provide the best bearing capacity on-site. In other words, our results indicate that the spiral pile will likely prove to be easily installed and have a large bearing capacity, if the shaft is given the optimal rotation when driving the pile and the shaft rotation is locked during the loading phase.

The rest of this section will summarize the observations of the density variation in the model ground after penetration tests using an X-ray CT scanner. The model ground was scanned initially before any tests were performed. The model pile was then installed to a total penetration depth of 130 mm, after which the model ground was again scanned to record the alteration of the ground after pile installation. The configurations of the X-ray CT scanner were a voltage of 200 kV, a current of 3 mA, an X-ray beam thickness of 2 mm, and a resolution of 2048 × 2048 × 1 voxels in each cross-sectional image. Fig. 10 shows a schematic view of the CT scanning depth. Arbitrary horizontal cross-sectional CT images are shown in Fig. 11, and Fig. 12 shows vertical cross-sectional CT images. Each CT image is constructed by combining a large planar distribution of CT values. Figs. 11 and 12 compare the altered areas around the piles under different rotary conditions. The green areas in each CT image

correspond to regions approximately maintaining the initial ground density (approximately 83% D_r). The blue areas represent low-density regions, which occur in very narrow zones along the pile surfaces in the case of Rot 100%, shown in Figs. 11(b) and 12(b). It is thought that the interactions between the soil and the pile surface were minimized in the case of Rot 100%, indicating that it is an optimal installation method. These results are similar to other findings about driving phases using different piles in previous research studies also using X-ray CT scans (Otani 2004, Taenaka 2007, Kikuchi 2008).

Conversely, the low-density regions were shown to exist continuously in a column shape around the spiral piles under the Rot 50% and Rot 200% conditions, as shown in Figs. 11(a) and (c), and 12(a) and (c). The borders of the low-density regions could be observed clearly in the case of Rot 200%. It is confirmed that the size of the low-density region is consistent along the longitudinal direction. It appears that the disturbed area surrounding the piles arose because the soil inside the pile column was forced upward. Further, the border of the low-density area could be observed as a gradation in the case Rot 50%. It was confirmed that the size of the low-density region was not consistent along the longitudinal direction in this case. This gradational low-density area was observed frequently in the CT images and shows that the dense sand was sheared and dilation occurred. It is reasonable to assume that the disturbed areas arose surrounding the pile because of the relative displacement of the sand between pile twists.

The red areas correspond to high-density regions, and a wedge can be seen below the pile tip under the Rot 50% and Rot 100% conditions in Figs. 11(a) and (b), and 12(a) and (b). In contrast, a high-density region did not appear near the tip of the pile under the Rot 200% condition, as shown in Figs. 11(c) and 12(c). It is presumed that one of the reasons that the bearing capacity was not improved was the over-rotation at a rate of 200%, which is why there is no high-density area under the tip of pile in this case, although it is usually observed.

5 CONCLUSIONS

The results obtained in this study can be summarized as follows:

1) The shaft rotary condition has a significant impact on the penetration resistance and the vertical bearing capacity of spiral piles. The optimal rotation condition decreases the penetration resistance and allows a large bearing capacity beyond historical penetration resistance values with little settling of the pile. When the spiral pile was driven at more than the optimum rotation ratio, the penetration resistance at the driving phase decreased. Further, the bearing capacity at the loading phase decreased as well. Therefore, it is necessary to determine the appropriate rotary condition and to perform execution management during actual operation when driving spiral piles.

2) The X-ray CT scanner is a powerful and effective apparatus to observe the internal ground alteration during penetration tests of unusually shaped piles, such as the spiral pile. The disturbance of the ground surrounding the pile was observed using CT images. It is thought that the interactions between the soil and the pile surface were minimized in the case of Rot 100%, indicating that it is an optimal installation method. Conversely, the low-density regions were shown to exist continuously in a column shape around the spiral piles under the Rot 50% and Rot 200% conditions. The border of the low-density area could be observed as a gradation in the case Rot 50%. This gradational low-density area was observed frequently in the CT images and shows that the dense sand was sheared and dilation occurred. It is reasonable to assume that the disturbed areas arose surrounding the pile because of the relative displacement of the sand between pile twists. Further, the borders of the low-density regions could be observed clearly in the case of Rot 200%. It appears that the disturbed area surrounding the piles arose because the soil inside the pile column was forced upward.

ACKNOWLEDGEMENTS

The authors would like to thank our student Mr. Etienne Bruchet for his great help for this research.

REFERENCES

1) Hirata, A., Kokaji, S., Fujita, M., Akamine, A., Fujita, M., Goto, T. (2003): Dilation stress in borehole induced by a spiral anchor, *Prceedings of the 3rd International Symposium on Rock Stress*, Balkema, Rotterdam, 499-505.
2) Hirata, A., Kokaji, S., Seung, K.S., Goto, T. (2005): Study on the estimation of the axial resistance of spiral bar based on interaction with ground, *Journal of MMIJ*, vol.121 370-377(in Japanese).
3) Isohata, H. (2003): Historical study on iron pile foundation and screw piles, *Journal of JSCE*, Vol. 2003, No.744, 139-150 (in Japanese).
4) Kikuchi, Y., Morikawa, Y., Sato, T. (2008): Plugging mechanism in a vertically loaded open-ended pile, *Proceedings of the Second BGA International Conference on Foundations*, ICOF2008. UK, June 2008. Vol.1, 169-180.
5) Otani, J. (2004): State of the art report on geotechnical X-ray CT research at Kumamoto University, X-ray CT for Geomaterials; Soils, Concrete, Rocks, 43-76.
6) Taenaka, S., Otani, J., Sato, T. (2007): Characterization of vertical bearing capacity of sheet-piles, *Journal of JSCE*, Division C, Vol. 63, No.1, 285-298 (in Japanese).
7) Yamashita, H., Hirata, H., Kinoshita, M. (2010): Challenges in the past and for the future of design and installation technologies on steel pipe piles in Japan, *Journal of JSCE*, Division F, Vol. 66, No.3, 319-336 (in Japanese).